Synthesis and functioning of SMART coatings for application in compact instruments and sensors

Henrik Fabricius
DELTA
Hjortekaersvej 99
DK-2800, Lyngby, Denmark
Fax (+45) 4587 0810, hf@delta.dk

Abstract

In the future the functioning of optical coatings will be ever more complex. Not only a specific transmission or reflection will be needed. The customers at the same time want extra features like a high laser damage threshold; a specific phase-retardation or a low group-delay dispersion and the desired functioning may be different in different spectral ranges. Such coatings typically end up consisting of all-different layer thicknesses and a mixture of both relatively thick and very thin layers. Advanced software and process systems are needed for the synthesis and production of this type of coatings. Both have been established at DELTA. The paper describes the synthesis and the functioning of different ultra hard SMART coatings, which are suited for application in compact instruments and sensors.

Introduction

The complexity of the functioning of the coatings increase for several reasons. First of all the construction of complex coatings is difficult to reveal and to copy by competitors and the application of a SMART filter in a product increases the lifetime of the product in the marked whereas the costs of the coating are limited. Another reason is the common marked trend to try to integrate the functioning of different devices into a single device in order to reduce the physical dimensions of the total product and the number of handlings required to assemble and adjust it. A further reason is the trend towards smaller dimensions of the optical components used in laser-based systems. Today optical filters often are laminated of a number of coated glass substrates. However, it is possible to reduce the physical dimensions of the filter, by combining the functioning of several of the coatings into a single advanced coating.

Optical coatings are often complicated thin-film structures consisting of a large number of sub-layers. More than 40 layers in an optical coating have become standard, within recent years. Until recently, complicated coatings were designed by optimisation of a good initial guess. This may be an easy or difficult task depending on the desired characteristics.

Edge-filters, notch-filters, mirrors, colour beam-splitters and band-pass filters are examples of widely used coatings that can be optimised from quarter-wave related stacks. The elimination of ripples in the pass-bands is mainly a question of obtaining a good adaptation between the multilayer and the surrounding media – and it depends mostly on the thickness of the outermost layers in the stack.

Band-pass filters are formed by inserting a layer, which have an optical thickness equal to an even number of quarter waves in a quarter-wave stack. Narrow banded filters may be obtained by combining several cavities. Making the initial guess for the optimisation of an advanced band-pass filter for DWDM (Dense Wavelength Division & Multiplexing), consisting of about 100 layers is not really a difficult task. The difficulties in this case are production-related.

It is much more difficult to guess the initial code for a coating having a performance very different from what we know from the classical filters. Such coatings typically end up consisting of

all-different layer thicknesses and a mixture of both relatively thick and very thin layers.[1] In the following this type of coatings are called SMART coatings.

At the moment (Spring '01) several SMART coatings consisting of more than 70 all-different layers are produced regularly by the thin-film group at DELTA.[2-4] The highest number of all-different layers deposited by the thin-film group at present is 128.[2]

To guess the code of such a SMART coating is impossible. A synthesis technique is needed for this purpose. In the 1980s, an approximate synthesis technique appeared. It was called the inverse Fourier transform technique.[1] This technique was implemented at DELTA in the period 1990 – 1993 and it was used to design some of the first SMART coatings produced at DELTA.[5,6,7] In literature, these coatings are known as quasi-inhomogeneous coatings.[8]

In the 1990s, another synthesis technique appeared. It is called the needle-synthesis technique,[9] and the DELTA thin-film group was among the first to implement this new technique in the period from 1993 to 1995. Today, the needle-synthesis technique is in daily use at DELTA.

The needle-synthesis technique is a powerful tool to design coatings with a sophisticated spectral performance. The disadvantage of the technique is mainly that it is difficult to manufacture the all-different layer structures designed.[3,4] Standard coating machines are not capable of doing this job. However, DELTA did successfully rebuild several systems to meet the requirements.[1,3,4]

A tight integration has been obtained between the design software and the software for the process system. This enables the deposition of complex coatings of all-different layer thicknesses as obtained by the synthesis with the needle technique. It is necessary to use optical monitoring techniques to control the deposition of a precision coating. The determination of the optimal steering wavelength for the process system is a difficult task when the coating is composed of all different thicknesses. A unique technique was developed for the automatic calculation of the steering wavelength for complex filters.[4]

The absorption of real coating materials is taken into account in the new designs.[1] It was common for many years to forget about the absorption in the coating materials, and it is actually acceptable in many cases. However, the increased number of layers in coatings makes it more important to include the absorption in the coating materials in the calculations. Furthermore, new applications appear in the ultra violet where the absorption is more pronounced. The absorption is introduced by substitution of the real refractive index by a complex refractive index. This is a very fundamental change and the consequences are large. Complex quantities appear everywhere in the calculations, which get much more complicated. However, the speed of the calculations performed by personal computers has increased even more recently, legalising it.

The large number of layers in the SMART coatings demands efficient tools for the optimisation. The classical first order optimisation is not sufficient anymore. During the period from 1998 – 2000, the author has put much effort into establishing procedures for second order optimisation of SMART coatings. A proper presentation of the mathematics involved is far beyond the scope of this paper. However, it is covered in detail in a large report from DELTA.[1]

The co-optimisation of several parameters for a SMART coating is the main subject of this paper.

The Merit function

The basis of all computer-based optimisations is a stepwise reduction of the deviation between a certain target and the estimated performance of a construction.[8,9] A single number describing the deviation is calculated with a merit function. It is common to apply Eq. (1) for the optimisation of a single property, u, at a fixed angle of incidence and s- or p-polarised light

$$F_u = \sum_{k=1}^{L} v(u_k)[u_k - \overline{u}_k]^{2p}, \quad p \in Z_+. \tag{1}$$

u, in example, could be the reflection of the coating at the L sampling points and $\overline{u}$ the corresponding desired target values. $v(u_k)$ is the spectral weighting of the sampling at λ_k. The merit function simply is the least-square deviation between the desired and the obtained characteristics, when p is equal to one. The sensitivity towards large deviations may be increased by application of a larger exponent $2p$ where p is a positive integer.

The dependence on the state of polarisation in general is taken into account by introduction of the following main expression[1]

$$F = \sum_{a=1}^{M} b_a [c_s F_{s-pol}(\theta_a) + c_p F_{p-pol}(\theta_a)], \tag{2}$$

where c_s is the relative weighting of the s-polarised light, c_p the relative weighting of the p-polarised light and b_a the weighting of the angle segment indexed a.

Co-optimisation of several properties

In the future, the functioning of optical coatings will be ever more complex. Not only a specific transmission or reflection will be needed. The customers at the same time want extra features like a high laser damage threshold, a specific phase retardation or pulse compression. In order to enable the co-optimisation of several parameters we introduce the following expression[1] describing the contributors for Eq. (2)

$$F_{x-pol}(\theta_a) = \sum_{m=1}^{N} c_m F_{m,x-pol}(\theta_a), \tag{3}$$

where c_m is the weighting of the contributor m and where x symbolises s or p. According to Eqs. (2) and (3) the merit function is composed of a number of additive contributions F_m and the first and second derivatives in respect to changes in the layer thicknesses do not cross-link. This means that we may discuss the calculation of each of the contributors F_m separately. This is done in detail in Ref. 1. In the following, we will try to co-optimise the reflection and the polarisation sensitivity as well as the reflection and the phase retardation introduced by different laser mirrors for 45 degrees of incidence.

First order optimisation (simplex type)

It is often possible to optimise the performance of the optical coating by changing the optical thickness of the layers forming the coating or alternatively by changing the refractive index of the layers. The coatings discussed in this paper are made of al-

ternating high and low indexed layers of two commercially available and characterised thin-film materials. The changeable quantities are: the total optical thickness of the coating, the thin-film materials, the number of layers in the multilayer and the thickness of the respective layers.

Once the materials, the total optical thickness and the number of layers are selected, a merit-function-based optimisation of the thickness of the layers is performed.[9] This is not a simple task and no unique solution exists to the problem. It is like searching for the deepest valley in the mountains. The initial choice of the total thickness, materials and the number of layers will place you somewhere in the landscape. You may then search for the bottom of the valley, but once you find it, you never really know whether it is possible to go deeper elsewhere in the same valley or in another valley.

The most common and widely used technique for optimisation of optical multilayers is the first order optimisation technique. The main idea is to calculate the first derivative or gradient vector

$$g(d) = \left(\frac{\partial F}{\partial d_1}, \frac{\partial F}{\partial d_2}, \cdots, \frac{\partial F}{\partial d_N} \right)^T, \tag{4}$$

and to search for the minimum in the anti-gradient direction

$$d_j \rightarrow d_j - \alpha \frac{\partial F}{\partial d_j} \Bigg/ \left| \frac{\partial F}{\partial d_j} \right|_{\max}, \tag{5}$$

where a is the step-length and according to Eqs. (1)-(3) we have

$$\frac{\partial F}{\partial d_j} = \sum_{a=1}^{M} b_a \sum_{u=1}^{N} c_u \frac{\partial F_u(\theta_a)}{\partial d_j}. \tag{6}$$

This technique is known as the steepest descent method or the simplex method.[1,10] Unfortunately, this technique is very slow in practice.[1,10,11] In the beginning, the convergence is fast, but later on, it becomes very slow. The problem is that the merit function possesses many locale minima, and the risk to end up in such a local minimum is pronounced.

Second order optimisation (Newton type)

Newton-type second order optimisation methods are usually much more efficient than any other method that does not utilise second order derivatives of the merit function.[1,10-12]

Finishing the optimisation of a coating, the following will be the case

$$F = 0, \quad \frac{\partial F}{\partial d_j} = 0, \quad \frac{\partial^2 F}{\partial d_i \partial d_j} = 0. \tag{7}$$

Assume for a moment that a first order optimisation has been used to reach a point in the neighbourhood of the minimum. The thickness of the layers in the multilayer at this time is given by

$$\mathbf{x}_0 = [d_1, d_2, \cdots, d_n]. \tag{8}$$

The first order derivatives of the merit-function at this time is known and kept in a gradient vector. The second order derivatives of the merit function are known too and we keep them in a two dimensional vector called the Hesse-matrix $\overline{\overline{H}}$. The matrix has n times n elements:

$$\overline{\overline{H}} = \begin{bmatrix} \frac{\partial^2 F}{\partial^2 d_1} & \frac{\partial^2 F}{\partial d_1 \partial d_2} & \cdots & \frac{\partial^2 F}{\partial d_1 \partial d_n} \\ \frac{\partial^2 F}{\partial d_2 \partial d_1} & \frac{\partial^2 F}{\partial^2 d_2} & \cdots & \frac{\partial^2 F}{\partial d_2 \partial d_n} \\ \vdots & \vdots & .... & \vdots \\ \frac{\partial^2 F}{\partial d_n \partial d_1} & \frac{\partial^2 F}{\partial d_n \partial d_2} & \cdots & \frac{\partial^2 F}{\partial^2 d_n} \end{bmatrix}. \tag{9}$$

According to Eqs. (1)-(3) and (6) the elements are calculated by

$$\frac{\partial^2 F}{\partial d_i \partial d_j} = \sum_{a=1}^{M} b_a \sum_{m=1}^{N} c_m \frac{\partial^2 F_m(\theta_a)}{\partial d_i \partial d_j}, \tag{10}$$

where b_a is the weighting of the different angular sections in case of non-collimated light and where c_m is the weighting of the different properties selected for optimisation, e.g. the reflection and the phase-retardation.

Performing a matrix-inversion on the Hesse matrix, it is possible to make a direct estimate of the optimal layer-code $\mathbf{x}_1$ as expressed by

$$\frac{\partial F}{\partial \mathbf{x}}\Big|_{\mathbf{x}_0} = \overline{\overline{H}} \cdot (\mathbf{x}_0 - \mathbf{x}_1) \Rightarrow \mathbf{x}_1 = \mathbf{x}_0 - \overline{\overline{H}}_{\mathbf{x}_0}^{-1} \frac{\partial F}{\partial \mathbf{x}}\Big|_{\mathbf{x}_0}. \tag{11}$$

In practice, it is recommendable to try to reach the solution at $\mathbf{x}_1$ in more than just a single step[12] as expressed by

$$\mathbf{x}_2 = \mathbf{x}_0 - (1 - c_x) \cdot \overline{\overline{H}}_{\mathbf{x}_0}^{-1} \frac{\partial F}{\partial \mathbf{x}}\Big|_{\mathbf{x}_0}, \quad c_x < 1. \tag{12}$$

In the design software, the merit is calculated at five different values of c_x (0, 0.2, 0.4, 0.6, 0.8) and a golden section search[13] and a final parabolic fit is used to determine the optimal value of c_x.

Sometimes the extreme point located by the calculations is a maximum instead of a minimum. In this case, it is necessary to step in the opposite direction, and use small steps initially as explained for the first order optimisation technique.

Second-order optimisation of optical coatings is much more efficient and much quicker than first order optimisation. This is especially the case when the number of layers is large and when close to the final solution. Introducing the second order optimisation in the TYNDFILM software, it turned out to be possible to further optimise most of the coating designs in use at DELTA. The ability to fully optimise a coating with a certain number of layers is especially important when the needle synthesis technique is applied.

The needle-synthesis technique

The needle-synthesis technique is an efficient design technique that was born in the late 1980s by two Russian scientists, Sh. A. Furman and Alexander V. Tichonravov.[9] I personally saw it for the first time when Alexander showed me the first version of his design software OPTILAYER in action in Canada in 1993.[8] Back in Denmark, the first parts of our new design program TYNDFILM were implemented. The idea of Furman and Tichonravov was to use the principles of optimal control theory[12] in order to solve the thin-film synthesis problem. The synthesis problem is a question of minimising a merit function. For this type of problem, it is possible to establish theorems; which set up the necessary conditions for the existence of an extreme in the form of Pontriagin's maximum principle.[12] It turns out that these theorems provide important conclusions about the optimum design of optical coatings.[14-16] One of the conclusions is that optimal thin-film structures consist of two materials only.[16] Another result tells us that: If it is possible to use several materials, the best results will be achieved when the largest and the smallest permissible refractive indices are used.[16] The description of the main concepts for the needle synthesis of two-material coatings can be found in Furman and Tichonravovs book from 1992[8] and the use of the technique is described in a number of papers.[11,16,17]

The main idea of the needle-synthesis technique is to scan a coating to find the best position to insert a needle layer of zero thickness and with the opposite refractive index. By insertion of the needle-layer, the number of layers in the coating increases by two, except for the situation where the needle is placed at the end of the multilayer.

First of all the physical thickness of the coating is divided into 1600 parts and the first-order derivative of the merit function in respect to a change of the thickness of the needle-layer is calculated in turn, by inserting a needle at the different positions. In each case the derivative is calculated for a needle with a shifted refractive index, $n(z)^+$, and for a needle with a non-shifted refractive index, $n(z)^-$. The best position to insert a needle layer is located by performing a plot of the following function, $P(z)$

$$P(z) = \frac{\partial F}{\partial d_j}\bigg|_{n(z)^+} - \frac{\partial F}{\partial d_j}\bigg|_{n(z)^-}. \qquad (13)$$

When the function $P(z)$ is negative at a position z, it means that the thickness of a needle inserted at this position increases when a merit function based optimisation is used to minimise the merit function F. The best position to insert a needle is found by identifying the position where $P(z)$ has the most negative value, see Fig. 1. It is not possible to obtain an improved performance by insertion of an extra layer when $P(z)$ is all positive. In this case, the total thickness of the coating must be increased.

The calculation of the $P(z)$ is equivalent to the calculation of the derivatives for a first order optimisation of a thin-film with a huge number of layers. Care must be taken to do the programming properly preserving time efficient calculations.

A new layer is only inserted when the $P(z)$ function is zero at all the interfaces between the sub-layers in the coating. A jump in the $P(z)$ value indicates that it is possible to further optimise the layer thicknesses. Although 1600 sampling points were used for the calculation of the $P(z)$ function shown in Fig. 1, it may be

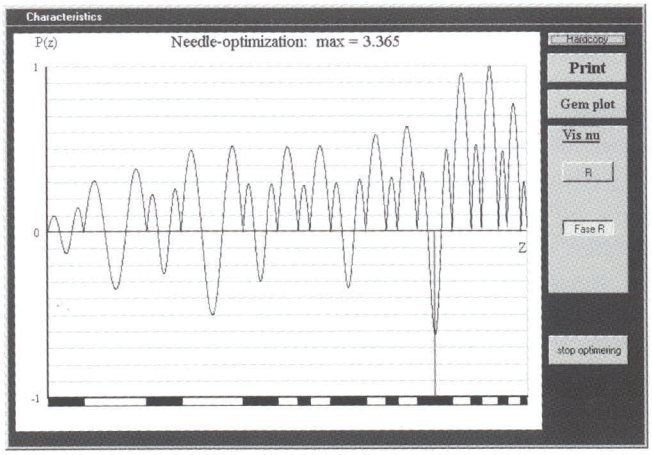

Fig. 1. Screen shot from the TYNDFILM programme. The structure with the black and white sectors at the bottom of the picture symbolises the coating. The P(z) function indicates the optimal position for the insertion of the next needle layer. The coating designed is a phase retarding mirror for a laser.

difficult to see whether the $P(z)$ value is exactly zero at the interfaces. The software performs a linear fit from each side and it calculates the intersection point.[1] The intersection points must be located within a small distance from the z-axis to allow the insertion of a new layer.

The first and second order optimisations described previously involve a simultaneous change in all layer thicknesses. This is not always optimal. Sometimes it is necessary to optimise the thickness of only a single layer to get free of a "trap". The $P(z)$ curve is a perfect tool for identifying the layers to optimise one by one.[1] The size of the discontinuities indicates how sensitive the thicknesses of the neighbouring layers are to changes. Furthermore, the sign of the $P(z)$ function indicates whether the thickness of the layers should be increased or decreased. The thickness must be increased when $P(z)$ is negative and decreased if it is positive.

Calculation of the derivatives

In most cases, it is possible to write the contributions to the merit function on the form shown in Eq. (1).[1] This is for example true for the transmission and reflection of light in the forward and backward directions and the corresponding phase shifts.

Performing a first order optimisation or a needle scan we need to calculate the first order derivative of F_u

$$\frac{\partial F_u}{\partial d_j} = \sum_{k=1}^{L} v(u_k) 2p (u_k - \overline{u}_k)^{2p-1} \frac{\partial u_k}{\partial d_j}. \qquad (14)$$

To perform a second order optimisation we also need to calculate the second order derivative

$$\frac{\partial^2 F_u}{\partial d_i \partial d_j} = \sum_{k=1}^{L} v(u_k) 2p(2p-1)(u_k - \overline{u}_k)^{2p-2} \frac{\partial u_k}{\partial d_i} \frac{\partial u_k}{\partial d_j} + \sum_{k=1}^{L} v(u_k) 2p (u_k - \overline{u}_k)^{2p-1} \frac{\partial^2 u_k}{\partial d_i \partial d_j}. \qquad (15)$$

The calculation of the first and the second order derivatives of u_k is not a simple task as u_k is a function of the matrix-product of as many complex matrices as layers in the coating. The calculation of u_k and the derivatives was shown in detail in a larger report[1] from DELTA. However, in this text we will limit ourselves to discuss the subject at a higher level.

Example 1: Designing a combined polarising beam splitter and mirror for a laser-diode

Polarising beam splitters usually are made in the shape of cubes. However, it is actually possible to design a single surface coating, which acts as a polarising beam splitter in a spectral range, which fits the tolerances on the emission wavelength of a laser diode. Figs. 2 and 3 show the transmission and reflection of a SMART coating; which works as a polarising beam splitter from 620 nm to 660 nm and as a highly reflecting mirror from 670 nm to 740 nm. The coating was designed by application of the needle synthesis technique and second order optimisation of the reflection and the transmission in the spectral range from 600 nm to 740 nm. The initial guess was composed of a high indexed layer of limited thickness and a thick low indexed layer. The number of layers in the final design is 53 and the coating is designed for ion-assisted deposition of TiO_2 and SiO_2. The absorption in the coating materials was taken into account and the reflection and the transmission was co-optimised by application of different targets for *s*- and *p*-polarised light. 'X' marks the desired transmission for the *s*-polarised light, whereas '+' marks the desired transmission of the *p*-polarised light in Figs. 2 and 3. The following merit-function was used for the optimisation

$$F = F_T + F_R. \tag{16}$$

The angular tolerance of the coating is approximately ±2 degrees in the polarising mode, whereas it accepts angles of incidence of −10 to +30 degrees in the reflecting mode. It is in example possible to use the polarising beam splitter for the excitation of the fluorophore[18] Cy5 at 650 nm and the polarisation independent reflection from 670 nm to 740 nm to reflect the emitted fluorescence.

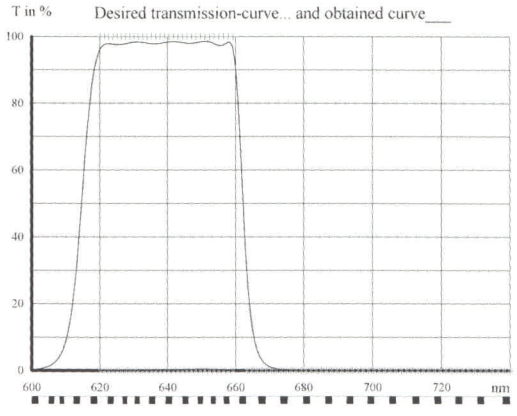

Fig. 2. 'X' marks the desired transmission for the s-polarised light, whereas '+' marks the desired transmission of the p-polarised light. The curves show the obtained transmission curves. Fig. 3 shows the corresponding reflection curves. The coating works as a polarising beam splitter from 620 nm to 660 nm and as a highly reflecting mirror from 670 nm to 740 nm. The number of layers is 53 and the coating is designed for ion assisted deposition of TiO_2 and SiO_2.

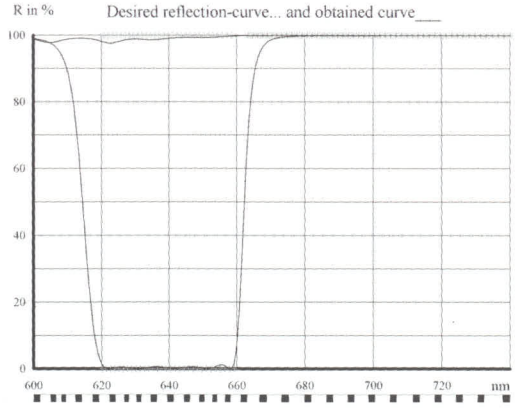

Fig. 3. 'X' marks the desired reflection for the s-polarised light, whereas '+' marks the desired reflection of the p-polarised light. The curves show the obtained reflection curves. A certain absorption in the TiO_2 layers accounts for the non-perfect reflection of s-polarised light and the non-perfect transmission of p-polarised light at wavelengths below 600 nm. It is important to co-optimise the transmission and the reflection to maximise the performance of the coating.

Optimisation of the phase retardation on reflection

During the interaction with a coating, a phase shift is introduced on the light. In general, this phase shift is different for *s*- and *p*-polarised light. This means that the state of polarisation may be changed during the interaction with the coating. Working with laser beams it is common to polarise the light parallel or orthogonal to the plane of incidence. In this case, phase retardation does not occur. This explains why most people forget about the phase performance in their daily work.

On the other hand, it is possible to utilise the phase retardation. For example, it is possible to design a coating that transforms a linearly polarised beam into a circularly polarised beam and it is possible to make the retardation independent of the wavelength in a certain spectral range.

Working with femtosecond lasers, the phase performance of the coatings suddenly become very important. The first, second and third order derivatives of the phase shift in respect to the angular frequency must fulfil certain requirements to suit the femtosecond laser system.[19-21]

Calculation of the phase shifts

The amplitude transmission and reflection coefficients are complex quantities, and we may write them on the polar form

$$r = \rho \exp(i\phi_r) \tag{17}$$

$$t = \tau \exp(i\phi_t), \tag{18}$$

where the quantities ϕ_r and ϕ_t symbolises the phase shifts resulting from the reflection and transmission of light in the boundary between the two media. Similar expressions exist for the reflection and transmission in reverse direction.

Writing the amplitude reflection or transmission coefficient as

$$\tilde{w}_k = w_{k1} - iw_{k2} \in [t, r, t_r, r_r], \tag{19}$$

where the index r refers to the reverse direction, it is possible to calculate the associated phase shift by

$$u_k = \tan^{-1}\left(\frac{-w_{k2}}{w_{k1}}\right) + 2\pi p_k, \tag{20}$$

where p_k is an integer and k the index of the sampling points. In a vector plot, u_k is a vector in the complex plan. This means that we have to add π to the result of a computer calculation of the $\tan^{-1}$ when the vector is inside the second or the third quadrant, and 2π if the vector is in the fourth quadrant. The optimal values of p_k are found by checking the characteristic for 2π discontinuities.

Optimisation of the phase-performance

We need to calculate the first and second-order derivatives of u in respect to the thickness of the layers. The first derivative is obtained by differentiation of Eq. (20)

$$\frac{\partial u_k}{\partial d_j} = \left[1+\left(\frac{-w_{k2}}{w_{k1}}\right)^2\right]^{-1/2} \frac{\partial}{\partial d_j}\left(\frac{-w_{k2}}{w_{k1}}\right)$$

$$= \left[w_{k1}^2 + w_{k2}^2\right]^{-1/2}\left[w_{k2}\frac{\partial w_{k1}}{\partial d_j} - w_{k1}\frac{\partial w_{k2}}{\partial d_j}\right], \tag{21}$$

where

$$\frac{\partial \tilde{w}_k}{\partial d_j} = \frac{\partial w_{k1}}{\partial d_j} - i\frac{\partial w_{k2}}{\partial d_j}. \tag{22}$$

The second-order derivative is found by differentiation of Eq. (21)

$$\frac{\partial^2 u_k}{\partial d_i \partial d_j} = 2\frac{\partial u_k}{\partial d_j}\left[w_{k1}^2 + w_{k2}^2\right]^{-1}\left[w_{k1}\frac{\partial w_{k1}}{\partial d_i} + w_{k2}\frac{\partial w_{k2}}{\partial d_i}\right]$$

$$+\left[w_{k1}^2 + w_{k2}^2\right]^{-1/2}$$

$$\cdot\left[\frac{\partial w_{k2}}{\partial d_i}\frac{\partial w_{k1}}{\partial d_j} - \frac{\partial w_{k1}}{\partial d_i}\frac{\partial w_{k2}}{\partial d_j} + w_{k2}\frac{\partial^2 w_{k1}}{\partial d_i \partial d_j} - w_{k1}\frac{\partial^2 w_{k2}}{\partial d_i \partial d_j}\right], \tag{23}$$

where

$$\frac{\partial^2 \tilde{w}_k}{\partial d_i \partial d_j} = \frac{\partial^2 w_{k1}}{\partial d_i \partial d_j} - i\frac{\partial^2 w_{k2}}{\partial d_i \partial d_j}. \tag{24}$$

Alternating optimisation of the phase retardation and the target

Optimising the phase retardation introduced by a coating, the shape of $\overline{u}(\lambda_k)$ may be unimportant. In this case, we will introduce the following modular phase targets

$$\overline{u}_s(\lambda_k) = B/\lambda_k + A, \tag{25}$$

$$\overline{u}_p(\lambda_k) = B/\lambda_k + A + C_R. \tag{26}$$

The optimal values of the coefficients A and B must fulfil the following requirements

$$\frac{\partial F_u}{\partial A} = 0, \quad \frac{\partial F_u}{\partial B} = 0. \tag{27}$$

Hence, A and B are found by calculation of

$$A = \frac{S_3 S_5 - S_2 S_6}{S_1 S_5 - S_2 S_6}, \quad B = \frac{S_1 S_6 - S_3 S_4}{S_1 S_5 - S_2 S_6}, \tag{28}$$

where

$$S_1 = \sum_{a=1}^{M} b_a \sum_{k=1}^{L} v(u_k)$$

$$S_2 = S_4 = \sum_{a=1}^{M} b_a \sum_{k=1}^{L} v(u_k)/\lambda_k$$

$$S_3 = \sum_{a=1}^{M} b_a \sum_{k=1}^{L} v(u_k)[c_s u_s(\lambda_k) + c_p u_p(\lambda_k) - c_p C_R]$$

$$S_5 = \sum_{a=1}^{M} b_a \sum_{k=1}^{L} v(u_k)/\lambda_k^2$$

$$S_6 = \sum_{a=1}^{M} b_a \sum_{k=1}^{L} v(u_k)[c_s u_s(\lambda_k) + c_p u_p(\lambda_k) - c_p C_R]/\lambda_k \tag{29}$$

The first part of the optimisation of the phase characteristics is obtained performing an alternating optimisation on the phase characteristics and the modular phase targets. However, it is recommended to fix the target curves as soon as they stabilise.

Example 2: Designing a quarter wave retarding laser-mirror

Fig. 4 shows the phase performance of a reflecting coating for 45 degrees of incidence. The coating works as a quarter-wave retarding laser-mirror in the wavelength range 650 nm ±25 nm. The reflection of s and p-polarised light exceeds 99.1% in the wavelength range from 600 nm to 740 nm, and the difference is approximately 0.1% in the wavelength range 650 nm ±25 nm, see Fig. 5. The phase retarding mirror may be used in combination with the polarising beam splitter in Figs. 2 and 3 to convert linearly polarised light into circularly polarised light. The wavelength ranges correspond well with the typical tolerance on the emission wavelength of laser diodes and the excitation and emission spectra of the fluorophore CY5.[18] The combined system of the two SMART coatings works as an optical isolator and a fluorescence separator. DELTA has got the necessary equipment to ultra hard coat the coating and cut them into pieces with a precision diamond saw. An obvious advantage of the system is the possibility to mount the parts without introducing any glue in the optical path, which may cause an extra phase-retardation due to double refraction. A disadvantage of the designed system is the need to rotate the phase retarding mirror to obtain an azimuth-angle[22] of 45 degrees.

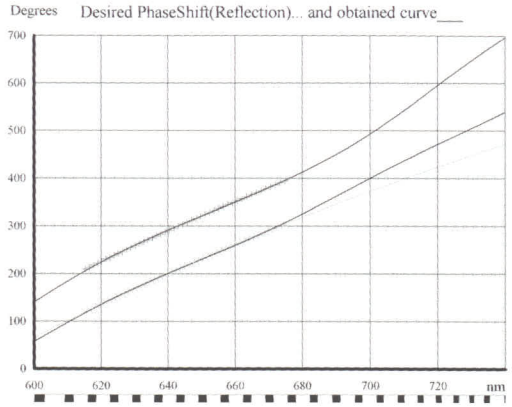

Fig. 4. Upper curve shows the phase shift associated with the reflection of p-polarised light whereas the lower curve shows the corresponding phase shift for the s-polarised light. The phase retardation is 90 degrees in the spectral range 650 nm ±25 nm. The coating is made of TiO_2 and SiO_2.

The applied phase targets were linear in frequency as expressed in Eqs. (25) and (26), and the desired phase retardation was $C_R = \pi/2$. During the first part of the needle synthesis, the phase targets were co-optimised. The initial guess was composed of a high-indexed layer of limited thickness and a thick low-indexed layer. The number of layers in the final design is 45 and the coating was designed for ion-assisted deposition of TiO_2 and SiO_2. The absorption in the coating materials was taken into account and the reflection and the phase retardation was co-optimised by application of different targets for *s* and *p*-polarised light. 'X' marks the desired transmission for the *s*-polarised light, whereas '+' marks the desired transmission of the *p*-polarised light in Figs. 2 and 3. The applied merit-function was composed as follows

$$F = F_R + 0.0253 F_{\phi_R}. \qquad (30)$$

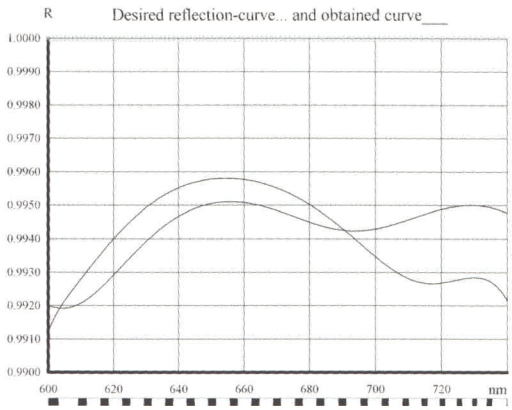

Fig. 5. Curves show the reflection of the phase retarding mirror at an angle of incidence of 45 degrees .The reflection of s and p-polarised light exceeds 99.1% in the wavelength range from 600 nm to 740 nm, and the difference is approximately 0.1% in the wavelength range 650 nm ±25 nm. The phase retarding mirror may be used in combination with the polarising beam splitter in Figs. 2 and 3 to convert linearly polarised light into circularly polarised light.

Example 3: Designing a laser-mirror with zero retardation

The two curves in Fig. 6 show the phase shifts on reflection of *s*- and *p*-polarised light in a laser mirror for a HeNe laser or a red laserdiode. The coating is composed of 30 layers. The phase shifts are almost equal and linear in frequency from 600 nm to 660 nm. Fig. 7 shows the corresponding reflection curves. The reflection of the *s*- and *p*-polarised light is slightly different. The overall reflection is approximately 99.4% in the spectral range 632.8 nm ±20 nm.

The applied phase targets were linear in frequency as expressed in the Eqs. (25) and (26) ($C_R = 0$). During the first part of the needle synthesis, the phase targets were co-optimised. The merit function was composed as in the previous example, see Eq. (30), and the weightings of *s*- and *p*-polarised light were even. The spectral weighting was 10 times larger in the range from 612 nm to 653 nm than outside this range.

The insensitivity towards the state of polarisation means that a linearly polarised laser beam remains linearly polarised, and that a circularly polarised beam remains circularly polarised, subsequent to a reflection in the mirror independently of the orientation of the laser. This may be of advantage in some sensor systems.

The wavelength range covered corresponds well with the typical tolerances on the emission wavelength of semiconductor laser diodes, for example those of a 635 nm laser diode.

The ultra-fast parameters

A short pulse can be seen as an amplitude-modifying envelope over a carrier. The carrier contains the phase information associated with the pulse, and it travels at a speed known as the phase velocity. However, the energy is clearly associated with the envelope travelling at a speed known as the group velocity.[19] Normally the group velocity is slower than the phase velocity, and the carrier appears to run through the envelope.[19-22]

Electromagnetic waves are additive. This means that we can Fourier decompose the pulse into a collection of monochromatic component waves with a continuous distribution of frequencies over a certain band. The phase of all the component waves matches each other at the centre of the pulse. In a dispersive medium,

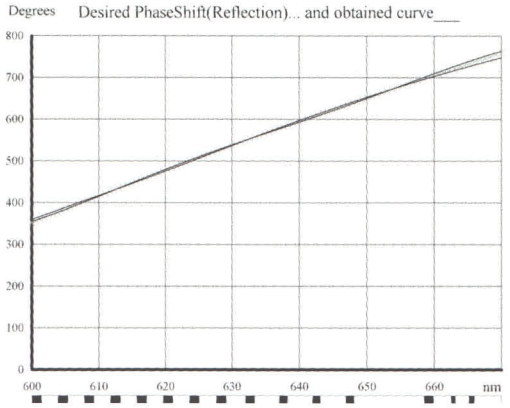

Fig. 6. The two curves show the phase shifts on reflection of s- and p-polarised light in a laser-mirror for a HeNe laser at 632.8 nm, or for a laser diode. The phase shifts are almost equal and linear in frequency.

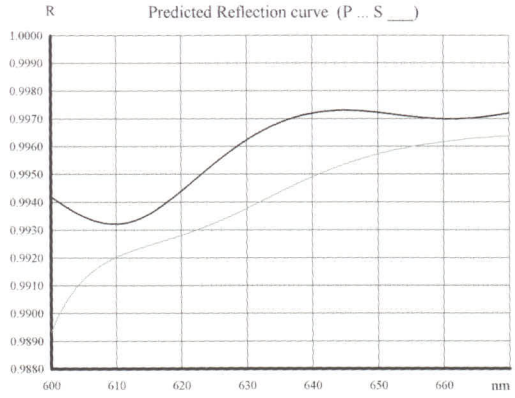

Fig. 7. The reflection of the s- and p- polarised light is slightly different. The overall reflection is approximately 99.4% in the spectral range 632.8 nm ±20 nm.

the component waves propagate with different speed. However, if the velocities are such that there is still a phase coincidence the pulse will exist there, unchanged in shape, although the carrier will be seen to have moved in respect to the pulse. No optical system exhibits a constant group delay over a large bandwidth. In general, the phase shift near some centre frequency ω_0 may be expanded in a Taylor series for frequencies near ω_0.

$$\phi(\omega) = \phi(\omega_0) + \frac{\partial\phi(\omega_0)}{\partial\omega}(\omega-\omega_0) + \frac{1}{2!}\frac{\partial^2\phi(\omega_0)}{\partial\omega^2}(\omega-\omega_0)^2 + \frac{1}{3!}\frac{\partial^3\phi(\omega_0)}{\partial\omega^3}(\omega-\omega_0)^3 + \cdots. \tag{31}$$

The first order derivative is called the group delay (GD).

$$GD = -\frac{\partial\phi}{\partial\omega} = \frac{\lambda^2}{a}\frac{\partial\phi}{\partial\lambda}, \tag{32}$$

where

$$a = 2\pi c, \tag{33}$$

where c is the speed of light in vacuum. The group delay represents a delay in the arrival of the pulse without change of shape. The second-order derivative is called the group-delay dispersion (GDD)

$$GDD = \frac{\partial GD}{\partial\omega} = -\left(\frac{2\lambda^3}{a^2}\frac{\partial\phi}{\partial\lambda} + \frac{\lambda^4}{a^2}\frac{\partial^2\phi}{\partial\lambda^2}\right). \tag{34}$$

It represents largely a broadening of the pulse. The third-order derivative is called the third-order dispersion TOD

$$TOD = \frac{\partial GDD}{\partial\omega} = \frac{6\lambda^4}{a^3}\left[\frac{\partial\phi}{\partial\lambda} + \lambda\frac{\partial^2\phi}{\partial\lambda^2} + \frac{\lambda^2}{6}\frac{\partial^3\phi}{\partial\lambda^3}\right]. \tag{35}$$

It is usually small, but if it is significant, it can adversely affect the shape of the pulse.

The thin solid curve in Fig. 8 shows the Group Delay Dispersion of a laser mirror in the spectral range 810 nm ±30 nm, which is comparable to the typical tolerance on the emission wavelength of high power laser diodes. The mirror, which is for normal incidence, consists of 25 layers of quarter-wave thickness, and it is made of TiO_2 and SiO_2. The thin solid curve in Fig. 9 shows the corresponding third-order dispersion. Both quantities are low and this is typical for a standard quarter-wave stack. The thin solid curve in Fig. 10 shows that the reflection of the mirror exceeds 0.9997 in the selected spectral range

Standing wave electric fields and laser damage threshold

Electric field rather than magnetic field is responsible for the interaction of light with matter, and so parameters like polarisation, amplitude reflection and transmission coefficients, and phase shifts are all understood as referring to the electric field of the wave.[23]

Two coherent waves having the same frequency and travelling in opposite directions in the same region of space, generates standing waves. In a thin-film stack, the waves reflected at each interface are coherent with the incoming wave, and therefore standing waves are set up in the coating. In instances where high power laser-beams are incident on a coating, the existence of these fields can play a vital role in determining whether the coating will survive the high power levels or not.[24-27]

Laser damage threshold

At the simplest level, laser-induced damage can be considered to involve the absorption of light and the subsequent heating of the material to some critical temperature at which failure occurs.[24]

The absorption of energy in an electromagnetic field is proportional to the time average of the square of the electric field (the standing wave electric field intensity), represented by $\langle E^2\rangle$, times the product of the index of refraction, n, and the absorption coefficient, α, at that point.

$$A = b_E n\alpha\left\langle E^2\right\rangle. \tag{36}$$

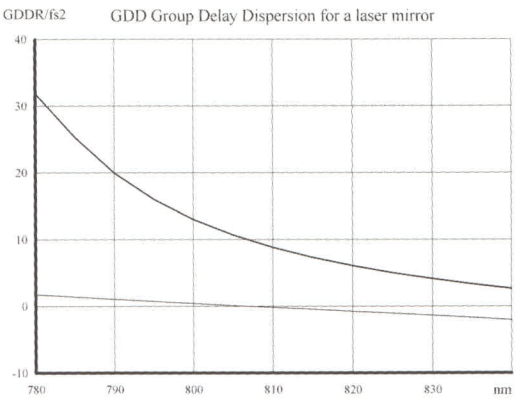

Fig. 8. Thin solid curve shows the Group Delay Dispersion of a twenty-five-layers QW-stack. The thick solid curve shows the increased GDD of the modified QW-stack, which was optimised in respect to the reflection and the intensity of the standing electric waves. Please notice the position of zero at the y-axis.

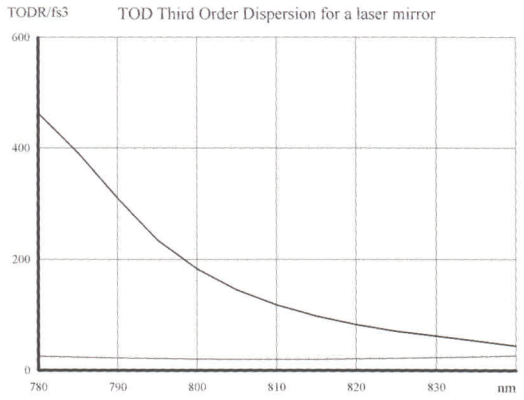

Fig. 9. Thin solid curve shows the Third Order Dispersion of a twenty-five-layers QW-stack. The thick solid curve shows the increased TOD of the modified QW-stack, which was optimised in respect to the reflection and the intensity of the standing electric waves.

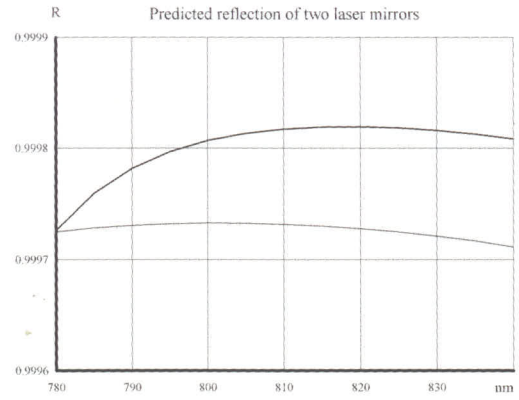

Fig. 10. Thin solid curve shows the predicted reflection of a twenty-five-layers QW-stack. The thick solid curve shows the increased reflection of the modified QW-stack, which was optimised in respect to the reflection and the intensity of the standing electric waves.

b_E is a proportionality constant. Generally, one considers the value of a constant through the volume of a film, but recent studies tend to indicate that the absorption is greater at interfaces than it is in the internal of the film.[25]

There are three main strategies for maximising the damage threshold of the optical coatings:

- Minimise locally high light intensities.
- Minimise the absorption coefficient of the material.
- Maximise the thermal or mechanical stability of the coating.[24]

It is important to minimise the electric field strength in layers with a high refractive index and a high extinction coefficient. Because high-index materials are generally believed to have lower damage thresholds than low-index materials, non-quarter-wave-layer designs generally involve a shift of the peak field into the low index material. In most practical modified quarter-wave designs, only the first two or four layer pairs are modified.[1,23]

An optimisation of the damage threshold of a coating typically involves the following steps:

1) Select a high-indexed thin-film material absorbing as little as possible. Fully oxidised Hafnium dioxide in this respect is a much better choice than Titanium dioxide.[28] However, on the other hand HfO_2 is more difficult to deposit.
2) Choose a deposition technique that guaranties a low defect density. Ion-assisted technique are not necessarily preferential in this respect.[28] Ion-beam sputtering is known to introduce defects.[26] Ion-assisted deposition may be of advantage depending on the parameters.
3) Minimise the maximal electrical field strength in the high-indexed layers.[25,27] The electric field strength often is maximal at the interface between two layers. This is especially critical because the density of defects is increased at the interfaces. It is evident from equation one that there are two reasons why the high indexed layers are critical: a) because the extinction coefficient is high, and b) because the refractive index is high.

Optimisation of the laser damage threshold

It is not a simple task to develop a strategy guaranteeing an increased laser-damage threshold. A reduced magnitude of $\langle E \cdot E^* \rangle$ in one layer does not necessarily mean that the maximal value of $\langle E \cdot E^* \rangle$ is reduced in the coating, and in practice the coating is damaged when $\langle E \cdot E^* \rangle$ exceeds a certain value.

The calculation of the total $\langle E \cdot E^* \rangle$ profile is slow due to the large segmentation of the total physical thickness of the coating and it is necessary to repeat the calculation for both states of polarisation, each angle of incidence and every wavelength.

The over-all merit function used for the optimisation is still the one shown in Eq. (3). However, performing a combined optimisation of the spectral performance and the laser damage threshold, the author proposed the following electric field specific contributor[1] $F_{m,x-pol}(\theta_a)$

$$F_{E_r,x-pol}(\theta_a) = \sum_{k=1}^{L} v_k(E) \int_{w1}^{w2} \left[\xi(\lambda_k, z_w) \left\langle E(\lambda_k, z_w) E(\lambda_k, z_w)^* \right\rangle \right]^{P_k} dz, \tag{37}$$

where

$$\xi(\lambda_k, z_w) = c_E \frac{2\pi}{\lambda_k} n(\lambda_k, z_w) \kappa(\lambda_k, z_w), \tag{38}$$

where $v_k(E)$ is the spectral weighting at the L wavelength forming the spectral curve. w1 is the index of the first sampling position z_{w1} in the layer. w2 is the index of the last sampling position z_{w2} in the layer. $n(\lambda_k, z_w)$ is the refractive index at the position z_w and the wavelength λ_k. $\kappa(\lambda_k, z_w)$ is the extinction coefficient at the position z_w and the wavelength λ_k. P_E is an exponent. It is possible to alter the sensitivity towards large values of the standing electric field (dielectric break down may occur) and large integral contributions (a thick layer absorbs more than a thin layer) by changing the value of P_E. In most cases, a value of in between 4 and 8 seems to be optimal. c_E is a constant factor, which we introduce to stabilise the precision of the calculation

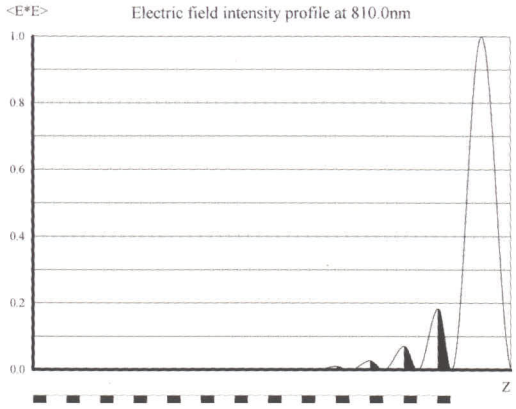

Fig. 11. The figure shows the time averaged square of the amplitude of the standing electric field in a twenty-five-layers QW-stack as function of the physical distance from the substrate. Black blocks and black filling indicate high indexed layers. The intensity peaks at the boundaries where the density of defects is high.

of Eq. (37) on a computer

$$c_E = \frac{\lambda_c}{2\pi n_H(\lambda_c)\kappa_H(\lambda_c)}. \qquad (39)$$

$n_H(\lambda_c)$ is the refractive index of the high indexed coating material at the wavelength λ_c and $\kappa_H(\lambda_c)$ the corresponding extinction coefficient. λ_c is centred on the wavelength range where the damage threshold is optimised (typically close to the wavelength of a laser).

The equations needed for a first and second order optimisation and needle synthesis coatings with an improved laser damage threshold were derived as part of a large report[1] and implemented in the TYNDFILM programme. However, it is outside the scope of this paper to discuss the subject in detail. We will limit ourselves to see the results of some calculations on a laser mirror.

Example 4: Designing a Twenty-five layer modified stack

Thin solid curve in figure 10 shows the reflection of a twenty-five-layer Quarter-wave stack for application at 810nm. The coating is made of TiO_2 and SiO_2. The Titania absorbs a small part of the light at this wavelength. Fig. 11 shows the standing wave electric field intensity as function of the physical distance from the substrate. Black blocks and black filling indicate high index layers. The standing wave electric field intensity in the air is shown for comparison. The peak value is approximately 4. It is evident that it is important to lower the intensity of light in the outermost high indexed layers.

The following combined merit function was used for the optimisation of the coating

$$F = F_R + 5\cdot 10^{-6} F_E, \qquad (40)$$

and the exponent P_E was set equal to 4 and the spectral contributions to F_E were limited to the wavelength range from 808 nm to 812 nm.

The standing wave electric field peaks at the interfaces between the layers in the QW-stack. This is critical because the density of defects is high there. Fig. 12 shows the corresponding plot for the modified quarter-wave-stack, and Fig. 13 shows the corresponding plot of the strength of the electric field (non-squared values). It is seen that the peak values of the standing wave electrical field intensities in the outermost high indexed layers are reduced, by shifting the peaks into the neighbouring low-indexed layers, which are believed to have a much higher damage threshold than the high indexed layers. The optical thickness of the outermost layer is 0.624 QW, whereas the thickness of layer number 24 is 1.551QW. The corresponding coefficients for the following pairs of layers are 0.773/1.424, 0.767/1.344, 0.846/1.217 and 0.905/1.122. Hence, a gradual transition occur towards the original QW thicknesses except for the thickness of the first layer, which in this case end up at a thickness of 3 QW.

The maximal standing wave electric field intensity was nearly reduced by a factor of two as result of the optimisation, and it is interesting to see from Fig. 10, that it even was possible to increase the average reflection in the investigated spectral range at the same time. However, it is evident from a comparison of the curves in the Figs. 8 and 9 that the data on the Group Delay Dispersion and the Third Order Dispersion are worse than prior to the optimisation. This shows that it is difficult to gain improvements in the laser damage threshold of the mirrors for an ultra fast laser system by optimisation of the layer thicknesses.

Conclusions

A structured merit-function was introduced, which enables a co-optimisation of the different properties of an optical coating. The principles of the first and second order optimisation and the needle synthesis were discussed and the developed techniques were applied on different coating examples. Equations were presented, enabling an efficient first and second order optimisation of the phase shifts introduced by optical coatings on transmission and reflection of light. Techniques for the alternating optimisation of the spectral curves and the phase targets was introduced and applied on different coating design. The subject of ultra fast optics was discussed and equations were derived for the calculation of Group Delay, Group Delay Dispersion and Third Order

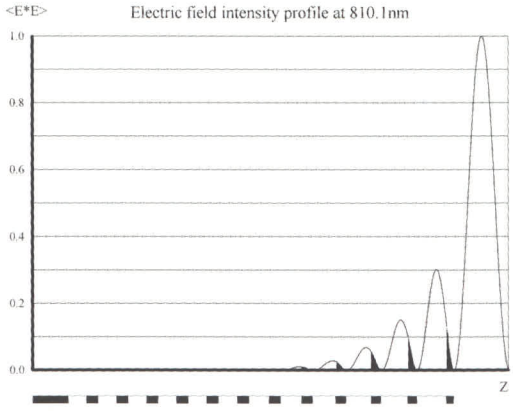

Fig. 12. The figure shows the standing wave electric field intensity in a twenty-five-layers modified QW-stack as function of the physical distance from the substrate. Black blocks and black filling indicate high indexed layers. The peak values of the electrical field intensities in the outermost layers are reduced, by shifting the peaks into the neighbouring low-indexed layers.

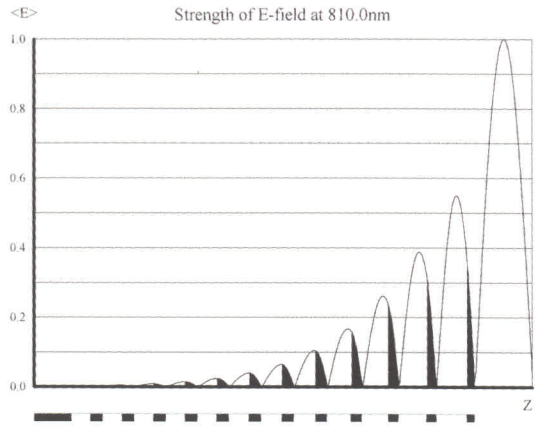

Fig. 13. The figure shows the strength of the electric field in the modified QW-stack shown in Fig. 12. Black blocks and black filling indicate high indexed layers.

Dispersion. The theory was applied on different examples. A combined polarising beam splitter and dielectric mirror was designed as well as a non-retarding mirror and a quarter-wave-retarding mirror for 45 degrees of incidence. A technique was proposed for the first and second order optimisation of the laser damage threshold. The versatility of the proposed method was illustrated by optimisation of a laser mirror.

References

1. H. Fabricius, *Design and Production of Ultra-hard Optical Thin-films,* DELTA report, 190 pages (December 2000).
2. H. Fabricius, *The gradient index filter – a new type of optical interference filter,* DELTA report, 100 pages (October 1992).
3. H. Fabricius, "Developments in the design and production of error-sensitive smart coatings", SPIE Proc. **2776**, pp. 58-69 (1996).
4. H. Fabricius, "Derivation of the steering wavelength for an optical monitoring system for the computer controlled deposition of ultra hard V-lambda filters", Northern Optics 2000 / EOSAM 2000 (p. 100), Uppsala, Sweden 6-8 June 2000.
5. H. Fabricius, "Gradient-index filters: designing filters with steep skirts, high reflection, and quintic matching layers", Appl. Opt. **31**, 5191-5196 (1992).
6. H. Fabricius, "Gradient-index filters: conversion into a two-index solution by taking into account dispersion", Appl. Opt., **31**, 5216-5220 (1992)
7. H. Fabricius, "The gradient index filter: An overview", DOPS-NYT 4-1996, 14-23 (1996).
8. H. Fabricius, "Closed loop optimization of quasi-inhomogeneous optical coatings", SPIE Proc. **2046**, 156-166 (1993).
9. Sh. A. Furman and A. V. Tikhonravov, *Basics of Optics of Multilayer Systems*, Chapter 1, Editions Frontieres, France, 1992.
10. H. M. Liddell, *Computer-aided Techniques for the Design of Multilayer Filters,* A. Hilger Ltd., Bristol, UK, 1981.
11. A. Tichonravov, and M. Trubetskov, "Thin film coatings design using second order optimization methods", SPIE Proc. **1782**, 156-164 (1992).
12. D. E. Kirk, *Optimal Control Theory – An Introduction*, pp. 344-347, Networks Series, Prentice-Hall Inc. 1970.
13. C. Holm, "Optical thin film production with continuous reoptimization of layer thicknesses", Appl. Opt. **18**, 1978-1982 (1979).
14. N. V. Grishina, and A. V. Tikhonravov, "Synthesis of optical coatings under oblique incidence of light using necessary conditions of optimality", Opt. Spectrosc. (USSR), **65**, 688-691 (1988).
15. A. V. Tichonravov, "On the optimality of thin-film optical coating design", SPIE Proc. **1270**, 28-35 (1990).
16. A. V. Tichonravov, "Some theoretical aspects of thin-film optics and their applications", Appl. Opt. **32**, 5417-5426 (1993).
17. A. Tichonravov, and M. Trubetskov, "Development of the needle optimization technique and new features of Optilayer design software", SPIE Proc. **2253**, 10-20 (1994).
18. W. T Mason, *Fluorescent and Luminescent Probes for Biological Activity,* Chapter 4, Academic Press, 1999.
19. "The ultrafast parameters", Macleod Medium **7**(4), December 1999.
20. A. V. Tikhonravov, M. Trubetskov, and A. A. Tikhonravov, "To the design and theory of chirped mirrors," Optical Interference Coatings, Technical Digest Series Vol. 9, pp 293-295 (1998).
21. F. Kartner, N. Matuschek, *et al.,* "Design and fabrication of double chirped mirrors", Opt. Lett. **22**, 831-833 (1997).
22. A. Yariv, *Optical waves in crystals*, J. Wiley (ISSN 0277-2493).
23. H. A. Macleod, "Thin-Film Optical Coating Design", p. 3, in *Thin films for optical systems* (ed. F. R. Flory), M. Dekker Inc., New York, 1995.
24. M. R. Kozlowski, "Damage-Resistant Laser Coatings," pp. 521-549, in *Thin films for optical systems* (ed. F. R. Flory), M. Dekker Inc., New York, 1995.
25. J. D. Rancourt, *Optical Thin Films User Handbook*, SPIE Optical Engineering Press,1996.
26. "Reaktives Ion-Plating-Verfaren zur Herstellung Dünner Schichten für die Optik", Balzers Applikationsbericht BB 800 031 AD (8901).
27. J. H. Apfel, "Optical coating design with reduced electric field intensity", Appl. Opt. **16**, 1880-1885 (1977).
28. C. J. Stolz *et al.*, "Advantages of evaporation of Hafnium in a reactive environment for manufacture of high-damage-threshold multilayer coatings by electron-beam deposition," SPIE Proc. **3738**, 318-324 (1999).
29. R. Szipöcs, "Theory and design of dispersive dielectric high reflectors for femtosecond pulse laser systems", Optical Interference Coatings, Technical Digest Series Vol. 9, 290-292 (1998).

About the author

Henrik Fabricius, M.Sc. (1986), Industrial Researcher (1988). Dissertation on r. f. sputtering of ZnO for UV-sensing. (the Danish degree as Industrial Researcher corresponds to the Danish Ph.D. degree Licentiatus). Graduated from the Technical University of Denmark, Physics Laboratory III, DK-2800 Lyngby. With DELTA Danish Electronics Light & Acoustics since 1988. Head of R&D, Optical Thin-film. Received the 1995 Annual Award of the Danish Optical Society for his research in the quasi-inhomogeneous optical coatings and the development of DELTA's new Gradient Index Filters. Board member of the Danish Optical Society since 1999.